City and Environment Interactions 4 (2019) 100029

Contents lists available at ScienceDirect

City and Environment Interactions

journal homepage: www.elsevier.com/locate/cacint

Research articles

Land cover change effects on land surface temperature trends in an African urbanizing dryland region

Felicia O. Akinyemi[a,b,*], Mphoentle Ikanyeng[b], Javier Muro[c]

[a] Geographies of Sustainability Department, Institute of Geography, University of Bern, Hallerstrasse 12, 3012 Bern, Switzerland
[b] Earth and Environmental Science Department, Faculty of Science, Botswana International University of Science and Technology, Private Bag 16, Palapye, Botswana
[c] Centre for Remote Sensing of Land Surfaces, University of Bonn, Genscherallee 3, 53113 Bonn, Germany

ARTICLE INFO

Article history:
Received 5 February 2020
Received in revised form 28 April 2020
Accepted 29 April 2020
Available online 11 May 2020

Keywords:
Land use
Land surface temperature (LST)
Normalized Difference Vegetation Index (NDVI)
Drylands
Peri-urbanization
Seasonal trend model
Small and medium-sized cities

ABSTRACT

Land use-land cover (LULC) association with land surface temperature (LST) is well known. Knowledge about land change effects on LST in urbanizing African drylands is very limited. We examined LST and vegetation variations in semi-arid Gaborone (Botswana's capital) using MODIS daytime and night-time LST (DNLST), and Normalized Difference Vegetation Index (NDVI) between 2000 and 2018. Significant land transitions were identified in the land cover change map using Change Vector Analysis of Landsat-based biophysical indices of vegetation, water and bare soil. Artificial surface and tree-covered areas were net gaining categories, whereas cropland and grassland were net losing categories. Detailed profiling of DNLST trends and breakpoints was conducted in five relatively homogenous sites representing land cover/transitions. Increasing NDVI and DNLST trends found were significant. Per class, LST change at daytime and night-time are as follows: built-up areas (1.8 K, 2.2 K), Gaborone dam (5.7 K, 0.2 K), settlement expansion areas (4.6 K, 2.2 K), and rural settlement (2.0 K, 1.5 K). The cooling effect of irrigation on daytime LST was higher than night-time LST as daytime LST trend as low as −0.4 K was found in areas of irrigated croplands. Validation with synoptic station temperature data and dam water levels provides empirical evidence that MODIS gave credible DNLST estimates in this urbanizing dryland area. Our results also suggest the role of climate variability in urbanizing drylands alongside land cover change in controlling the LST. Regardless, coupling DNLST and land cover changes can provide useful information for spatial planning of drylands to create smart cities that are resilient to climate change.

1. Introduction

Land use-land cover change (LULCC) as an environmental change driver plays an important role in modulating the local microclimate including land surface temperature (LST), especially in urbanizing areas [1–3]. Although the product of natural and anthropogenic factors in increasingly globalized land systems, a region's LULCC mainly reflects the heightening socioeconomic transformations due to human activities [4–7]. Alterations of urban landscape composition and configuration due to LULCC as well as the biophysical context (e.g. topography) affect LST [8,9]. In urbanizing regions, natural and semi-natural land covers of mostly rural landscapes are replaced increasingly with concrete and other construction materials. Urban LST estimation is complicated due to the surface heterogeneity occasioned by the different land covers and mixed uses. This is because land surface emissivity is highly variable and can vary over short distances [10]. Information about land change impacts on urban LST is needed for the proper design and spatial planning of smart cities in the face of climate change. For example, when seeking to mitigate overheating in city designs that can cause heat stress-related illnesses among urban dwellers [11–13]. Ameliorating extreme temperatures is an issue of increasing concern for urban areas worldwide [14].

Most studies investigating LST in the global south have concentrated on megacities and there are only a handful of such studies conducted on African cities. Examples are Freetown and Bo, Sierra Leone [15]; Warri, Benin-City and Port Harcourt, Nigeria [16]; Onitsha, Nigeria [10], Harare, Zimbabwe [17]. Other studies have focused on river basins such as the Inner Niger Delta, Mali [18], and the Kilombero catchment, Tanzania [19]. Relatively little is known about land change impacts on LST in emerging cities in comparison to the megacities, hence the need to fill this gap. By emerging cities, we refer to small and medium-sized cities with a million or fewer inhabitants [20]. Knowledge about LST and its interaction with land change in African emerging cities in dryland regions is also grossly lacking. Drylands are regions classified climatically as arid, semi-arid, or dry sub-humid, and are characterized by high variability in both rainfall amounts and intensities [21]. Faced with pressures from environmental change, emerging cities in all regions of the world are required to be resilient as more people will live there and projected future urban growth is mostly to occur in this type of cities [9,10,20,22–24].

* Corresponding author at: Geographies of Sustainability Department, Institute of Geography, University of Bern, Hallerstrasse 12, 3012 Bern, Switzerland
E-mail addresses: felicia.akinyemi@gmail.com, (F.O. Akinyemi), mphoentle.ikanyeng@studentmail.biust.ac.bw, (M. Ikanyeng), jmuro@uni-bonn.de. (J. Muro).

http://dx.doi.org/10.1016/j.cacint.2020.100029

This study examined the effects of urban land change on LST trends in Gaborone, a dryland region in Botswana. Although many factors influence LST and these are quite complex in dryland contexts, we focused on examining how LULCC is associated with LST, as the former is fundamental in capturing anthropogenic influences. Not much is known about the long-term spatiotemporal variation of LST and the influence of LULCC in semi-arid and arid regions [25]. Unlike many LST related studies examining the effects of specific land transitions such as deforestation, we examined the effects of all types of urban land transitions as well as areas where land cover persisted, i.e. remained unchanged. Trends in LST and vegetation conditions, as well as their relationships with land cover, were analyzed using long-term satellite time-series data from MODIS between 2000 and 2018. There are not many studies utilizing remotely sensed time-series such as MODIS and Landsat to understand the relationship between LST and land cover (e.g. [15,26,27]). With its very high temporal resolution, we investigated how useful MODIS datasets are for assessing LST and vegetation changes with land change in urban dryland contexts. MODIS products are mostly used for global and regional studies because of the coarse spatial resolution [28]. Analyzing LST's relationship with vegetation is also important as vegetation cover is a major predictor of urban LST [9,29]. Jonsson [29] found that vegetation was a major factor influencing the climate over Gaborone.

As LST varies with time of day [12,25], we also compared daytime and night-time LST trends over Gaborone. Questions answered in this study include LST changes over the 18-year study period, and how these relate to LULCC in an urbanizing dryland context. As dryland environments are highly sensitive to human and natural perturbations [30], improved understanding of LST interactions with urban land change can better inform city adaptation to environmental change, particularly climate change in drylands.

2. Materials and methods

2.1. Study area

The study area located to the southeast of Botswana comprises Gaborone City (the capital of Botswana), and its immediate surrounding settlements (Fig. 1). The immediate surroundings are important for consideration of urban land change as the city is expanding into these peri-urban areas.

With an average altitude of 1014 m a.s.l., the Gaborone region as defined in this study is positioned between the Kgale hill in the southwest and Oodi hill to its northeast and extends to the southern tip of the Gaborone dam. Drained mainly by the Notwane River and the Segoditshane River, the region is largely dependent on water availability from the reservoir. As a dryland region, the dam's reduced water level over time negatively impacts the city and that of nearby settlements. With incessant water shortages in Gaborone, the North-South Carrier (NSC) water scheme was implemented to transport water 360 km to Gaborone from the Letsibogo and Dikgatlhong dams located northwards [31,32].

The climate of the city is semi-arid, hot steppe (Köppen's BSh classification) with annual rainfall ranging between 475 and 525 mm. Temperatures are highest in summer (October to March) with a daily minimum and maximum of 19 °C and 40 °C respectively and night-time temperature occasionally drops below 0 °C in Winter [33]. Due to net in-migration, Gaborone, as the financial, administrative and educational nerve center of Botswana, is fast growing into a primate city from 3855 inhabitants in 1964 to 231,592 in 2011 [34,35]. As the number of inhabitants increases, the higher the water consumption level and it is difficult though to decouple the consumption of water from variations in precipitation.

2.2. Data

MODIS land surface temperature (MOD11A2.006 LST_Day_1km and LST_Night_1km) and MODIS Normalized Difference Vegetation Index (NDVI) (MOD13Q1.006, 250 m) time series data were used to analyze LST and NDVI trends over Gaborone. The full archive of images available from July 2000 to June 2018 was used. The MODIS LST and NDVI datasets are preprocessed by taking into cognizance clear sky conditions and cloud pixel masking [12]. MODIS has been widely used in studies examining LST as the data series are standardized [36–40]. Several studies have also found that NDVI captures the temporal changes in vegetation and positively

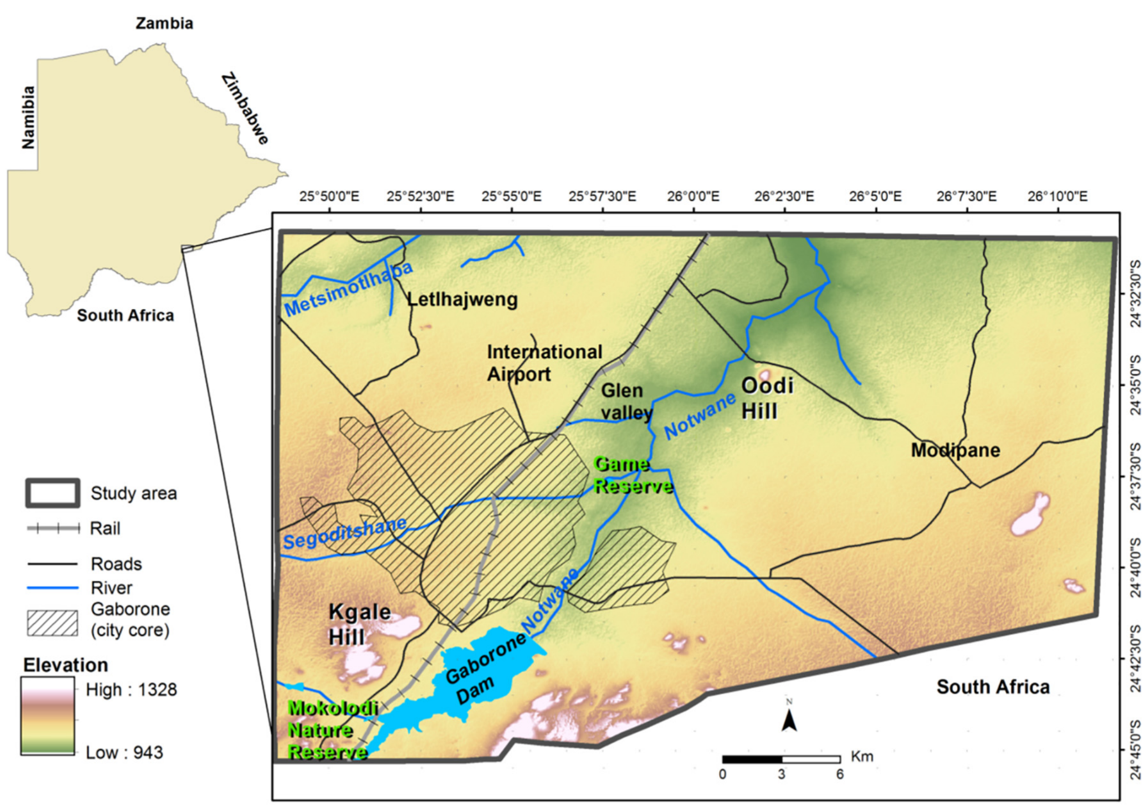

Fig. 1. Study location Gaborone in southeast Botswana.

correlates with precipitation and temperature although with notable lags [41,42].

The RCMRD/SERVIR Greenhouse Gas Inventory (30 m) land cover data (GHG-LULC) for Botswana of the year 2000 was utilized in this study [30]. For 2018, a land cover map was produced based on Landsat 8 images (30 m) with 85% classification accuracy.

Temperature data from the Sir Sereste Khama International Airport (SSKA) synoptic station was obtained from the Botswana Department of Meteorological Services. It was utilized in this study to compute the trend in comparison with outputs from MODIS LST products. The Gaborone dam's water level data was used to compute trend and ascertain its relationship to LST. The water level in the dam is monitored regularly.

2.3. Methods

2.3.1. Analysis of LST and NDVI trends

To examine how land cover transitions affect LST in the Gaborone region, we first analyzed and mapped the changes in LST assuming monotonic trends over the 18-year study period. Afterward, changes in LST were analyzed for breakpoints. The R package Greenbrown was used to analyze LST, NDVI trends and breakpoints [43]. The Seasonal Trend Model (STM) used as implemented in this package is based on the additive decomposition model [44]. Linear and harmonic trends are fitted to the original series using an Ordinary Least Squares (OLS) regression, and a Mann-Kendall test is used to determine the significance of the trends found. Analyzing LST for a breakpoint is important, particularly in drylands where abrupt changes caused by disturbances (e.g. deforestation, fires, drought and floods) are common [43,45]. To examine the influence of abrupt changes, the maximum number of breakpoints is set. A breakpoint in the time series data is detected by searching for structural changes in a regression and the position is estimated by minimizing the residual sum of squares [43]. The trend is split into two segments when a breakpoint is detected, and the significance of the segment slope is determined.

A STM generally shows more robust results than aggregation methods such as the OLS regression over annual means due to the higher availability of data points [19,43]. Linear regression is used to rescale the slopes of the trends into LST change in Kelvin (K) for better interpretation of results as in Eq. (1) [19]:

$$LST = slope * time + intercept \tag{1}$$

Results were afterwards classified into significant and non-significant trends at the 90% confidence level.

2.3.2. Land use-land cover change analysis

The cover maps for 2000 and 2018 utilized the same classification scheme (Table 1) based on the Intergovernmental Panel on Climate Change (IPCC) and United Nations Convention on Combating Desertification land use legend [46–48]. The six classes contained in the scheme are (1) tree-covered area, (2) grassland, (3) cropland, (4) waterbody, (5) artificial surface area (e.g. settlement) and (6) otherland.

The accuracy of both the 2000 and 2018 maps have been independently assessed. The Botswana 2000 GHG-LULC map was produced from Landsat 5 and 7 images and validated through field verification by the Botswana Department of Survey and Mapping (DSM). The 2018 cover map was based mainly on Landsat 8 image data. The accuracy attained for the 2018 cover map was 85% using ground reference data of land cover samples collected during fieldwork in 2018 and high-resolution images in Google Earth Pro, as well as correction applied to misclassified pixels based on official and well established external data (e.g. Waterbody vector data from DSM).

For detecting LULCC in the study area, the post-classification bi-temporal comparisons (PCC) method was used [49]. This method aligns independently classified images of two-time points on a per-pixel basis to detect where changes occurred between the dates [50]. The detected changes form the basis for quantifying the area, i.e. the amount of land involved, in the "from-to" change matrix of transitions among land classes. The output from the change detection process is necessary to establish an association with LST. PCCs are often prone to error propagation [51], where the errors from the maps of the first and second periods are accumulated. To minimize error propagation in the PCC, we performed a Change Vector Analysis – CVA [52]. CVA provides information on the magnitude and the direction of the change, i.e. the intensity and the spectral behavior of the change vector respectively [53]. The CVA was executed over two multitemporal composites of Landsat images for 1999–2001 (Landsat 7), and 2016–2018 (Landsat 8). These composites contained the percentile 90 of the normalized difference indices of vegetation (normalized difference vegetation index – NDVI, [54]), water (normalized difference water index – NDWI) [55] and bare soil (normalized difference built-up index – NDBI, [56]). Maxima metrics of these indices have been shown to better capture the biophysical conditions of the land surface [57] and significant land cover changes are expected to produce variations in these metrics. To separate significant from non-significant changes, we applied a histogram-based thresholding technique to the magnitude of the CVA [53,58]. Pixels with low magnitude values were masked out from the PCC, and the change direction of the remaining pixels was used to analyze the land cover transitions of the PCC.

Table 1
Land cover classification scheme used in the study.

Land classes	Description
Tree-covered area	An area covered with trees such as sparse, moderate forest and/or woodland.
Grassland	A land area covered predominantly with grass and shrubs such as closed grassland, open grassland, closed shrubland, and open shrubland.
Cropland	An area of crop growth usually irrigated or rainfall dependent.
Waterbody	Naturally formed water coverage on the earth surface such as wetland, river or manmade such as dams.
Artificial surface area	The land area of infrastructure and human settlements comprising buildings, i.e. commercial, residential, industrial, and roads/streets.
Otherland	Includes barelands such as exposed land surfaces void of vegetation, rocky outcrops, dunes, and mining area.

The significant land cover transitions were aggregated into cropland expansion areas, forestation, deforestation, and settlement expansion areas to better interpret their association with LST and NDVI trends. We also compared LST and NDVI trends over areas of persistence, i.e. no change. The very small change areas, each covering $< 1\%$ of the total land area, were combined and labeled as other transitions. This aids separating the urbanization effect on LST into these individual land transition types. Validating urban LST values derived from Remote Sensing (RS) is not straightforward because the derived LST is representative of the whole pixel, whereas field-based temperature measurements are point-based and LST can vary over short distances [10]. With these fine-grain data requirements of heterogeneous cityscapes [14], field validation of RS-derived LST in urbanizing regions is only meaningful over homogeneous areas [10,59]. LST daytime and night-time data were extracted over five sites (A to E) with relatively homogenous LST patterns. These selected sites represent different land cover and/or transition areas such as abandoned croplands with overgrowths, forest, waterbody, urban and rural settlements in the study area.

3. Results

3.1. Land cover change

LULCC over the 18-year study period in Gaborone was analyzed to identify and quantify the amount of land involved in land transitions from one class type to another. The share of land under each land transition type by class is shown in Table 2, and Fig. 2 depicts their spatial distribution. The most notable land covers in Gaborone in terms of their share of land were: artificial surface areas such as settlements, that increased from 108.48 km^2 (12.26%) in 2000 to 222.98 km^2 (25.21%) in 2018; tree-covered areas consisting of deciduous trees and woodlands increased from 100.8 km² (11.40%) in 2000 to 210.23 km² (23.77%) in 2018; grassland including shrubland decreased from 627.27 km² (70.92%) in 2000 to 421 km² (47.6%) in 2018; and cropland, which lost half its size as it reduced from 24.45 km² (2.76%) in 2000 to 12.82 km² (1.45%) in 2018.

Fig. 2(a, b) shows the losses and gains in areas of significant land cover changes over the study period. The amount of land share among categories in 2000 and 2018 is available as Fig. S1 (listed as supplementary information). The change budget quantified the amount of land area gained, lost and persistent among land cover classes between 2000 and 2018 (Fig. 2c). Persistent land covers amounted to 89.31% of the total land area. Artificial surface and tree-covered areas are net gaining categories, whereas cropland and grassland are net losing categories during the 18-year study period. The spatial extent of waterbody representing the Gaborone dam fluctuates with the water level.

3.2. LST trends

LST trends during the daytime and night-time were analyzed using the STM for the period July 2000 to June 2018 as shown in Fig. 3. LST patterns were examined in five sites (A to E) selected to represent different land transitions and persistent land cover areas of importance in the study area (see Table 3 for a detailed description of each site).

Significant increasing trends in daytime and night-time LST were found over the study area. Daytime LST increase was highest over the Gaborone dam (site A, min 2.6 K, max 5.7 K). The LST trends at night-time, however, are reversed as the dam showed a significant decrease when compared to the daytime LST (min −1.2 K, max 0.2 K), whereas significant increases were mostly found over the built-up areas in Gaborone (site C, min 0.8 K, max 2.2 K). Daytime LST increase was lower over the built-up (min 0.1 K, max 1.8 K) than over the surrounding rural settlements (e.g. site E, min 1.2 K, max 2.2 K) or the settlement expansion areas (min 0.3 K, max 4.5 K). LST trends increased but remained very low over urbanizing areas (e.g. site D, daytime - min 0.3 K, max 0.8 K; night-time – min 0.5 K, max 0.9 K). LST trends varied over cropland areas depending on whether it is an area of abandoned croplands (e.g. site B, daytime – min 0.8 K, max 1.3 K; night-time – min 0.8 K, max 1.1 K), or irrigated (daytime – min −0.4 K, max 0.4 K; night-time – min 0.9 K, max 1.0 K). Detailed examination of LST trends entailed individual profiling of the five sites (A–E, Fig. 4).

Fig. 4 depicts daytime and night-time LST trends and breakpoints for the selected sites. Daytime and night-time trend breakpoints detected for years 2005 and 2013 over the Gaborone dam (representing waterbody) (Fig. 4a) are well captured in the dam water level data depicted in Fig. 5. Fig. 5 shows fluctuations of the Gaborone dam water level over the study period. LST patterns over the Gaborone dam match the periods of drought and non-drought conditions as the temperature peaked at lower water levels (Fig. 5) and the temperature dropped when the dam flooded.

The LST trend breakpoints captured the low water level in the dam in 2005 and 2013–2014 (Figs. 4a, 5). The water level in the dam is negatively correlated to daytime LST. The daytime LST trend shows an increase over the dam, whereas the dam's water level shows a decreasing trend. The latter is confirmed as the dam's water level dropped from 121.8 m³ in 2000 to 93.1 m³ in 2018. For the other four sites (Fig. 4B–E) only one breakpoint in each is detected with significant trends in 2007 for daytime LST and in 2006 for night-time LST. LST patterns over these four sites were similar before and after the breakpoints.

3.3. Relationship between LST, NDVI, and LULCC

Changes in daytime LST, NDVI and land cover in Gaborone over the 18-year study period are shown in Fig. 6. Descriptive statistics such as the minimum (min), maximum (max), mean (μ) and standard deviation (σ) give further insight into the variations in LST and NDVI trends by land transition types over the study area (Table 4).

Maximum daytime LST increase was highest over the Gaborone dam. In the case of night-time LST we see the opposite patterns; decreasing trend over the dam and increasing trend over the urban built-up core areas (Fig. 6a, d). These areas have not experienced land cover changes during the study period. In terms of land change (Fig. 6c), significant increases in the daytime and night-time LST were found in deforested areas.

Areas of significant increasing NDVI trends corresponded to areas that experienced forestation such as gallery vegetation found around the dam, along the river courses and irrigated gardens. Increases in LST over areas of cropland expansion were similar during daytime and night-time and although NDVI increased, it was low. Maximum LST (daytime and night-time) increased over areas of settlement expansion. Although NDVI decreased in most areas of settlement expansion (Fig. 6b), there was a significant increasing NDVI trend in a few settlement expansion areas. In areas of persistent land cover, the increase in daytime LST was higher than in night-time LST. NDVI experienced overall increasing trends over the study area.

4. Discussion

Several studies have examined the influence of urban land cover change and LST trends. Most of these studies focus on short-term spatiotemporal patterns such as the annual temperature cycle, the urban heat/cool island (UHI/UCI) phenomena, and often do not use dense satellite image time-series as was done in this study [66,67]. While many studies have focused on large megacities, little is known of the effects of land cover change on the LST of urbanizing rural settlements in peri-urban areas, and emerging cities, particularly in drylands. These small to medium-sized cities are important as they are expected to absorb a larger proportion of the growing urban populations than megacities in the coming years [20].

4.1. Urban land change

An important land cover change noticeable in the Gaborone region is the expansion of human settlements, particularly built-up areas of Gaborone city into the surrounding rural areas. Urban expansion occurred mainly in the western part of the region, northwest with some patches towards the north. This can be mainly attributed to population growth due to an influx of people into Gaborone from all parts of Botswana. While undeveloped, the areas west of the rail (refer to Fig. 1) were mostly used for

Table 2
LULC change matrix over the study period.

2000 land cover	2018										2000 total	
	TC		G		C		W		AS			
	km²	%	km²	%	km²	%	km²	%	km²	%	km²	%
TC	**60.55**	**28.80**	27.35	6.50	0.28	2.16	0.06	0.33	12.57	5.64	100.80	11.40
G	146.52	69.70	**368.92**	**87.63**	8.41	65.58	0.45	2.58	102.97	46.18	627.27	70.92
C	0.65	0.31	17.55	4.17	**2.79**	**21.77**	0.003	0.02	3.45	1.55	24.45	2.76
W	1.59	0.76	1.96	0.47	0.47	3.67	**16.91**	**97.08**	2.52	1.13	23.46	2.65
AS	0.92	0.44	5.22	1.24	0.87	6.81	0	0.00	**101.47**	**45.50**	108.48	12.26
2018 Total	210.23		421.00		12.82		17.42		222.98		884.45	
2018 (%)	23.77		47.60		1.45		1.97		25.21			

Note: Persistence is shown in bold. TC – Tree-covered area, G – Grassland, C – Cropland, W – Waterbody, AS – Artificial surface area.

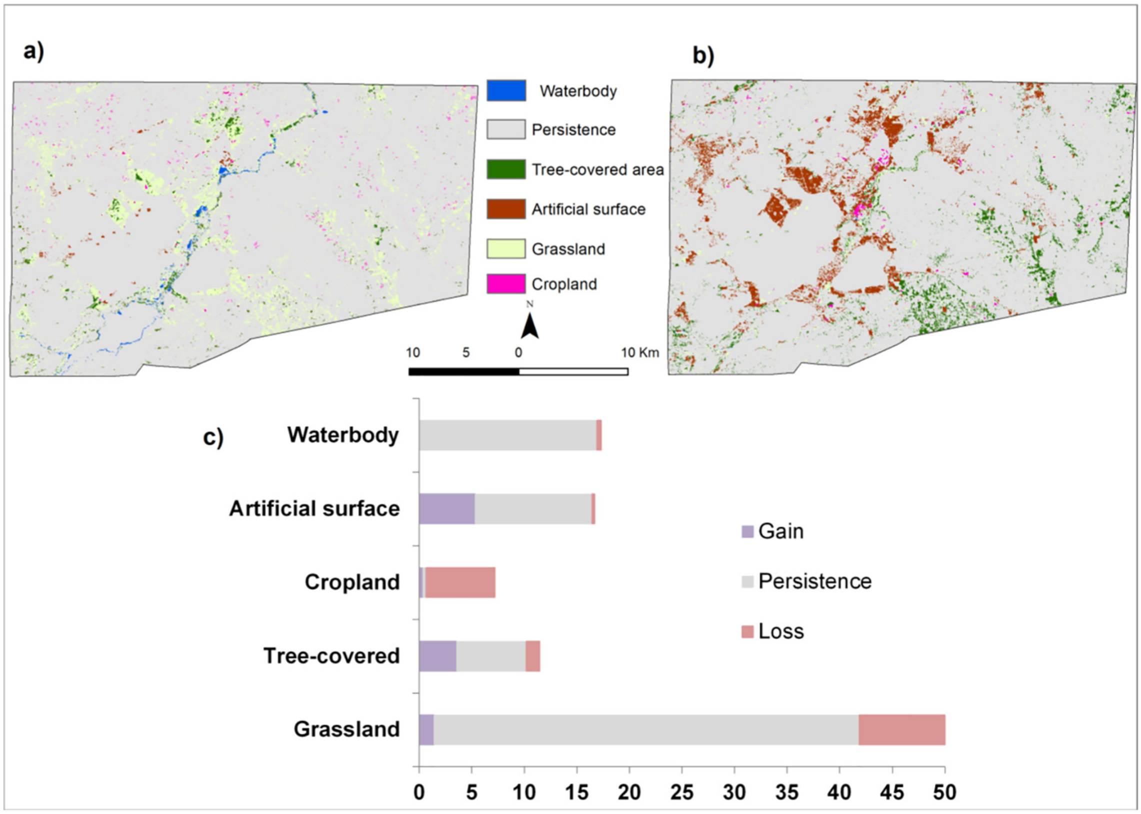

Fig. 2. Land cover change during 2000–2018, a) losses and persistence, b) gains and persistence, c) change budget (percent of the study area).

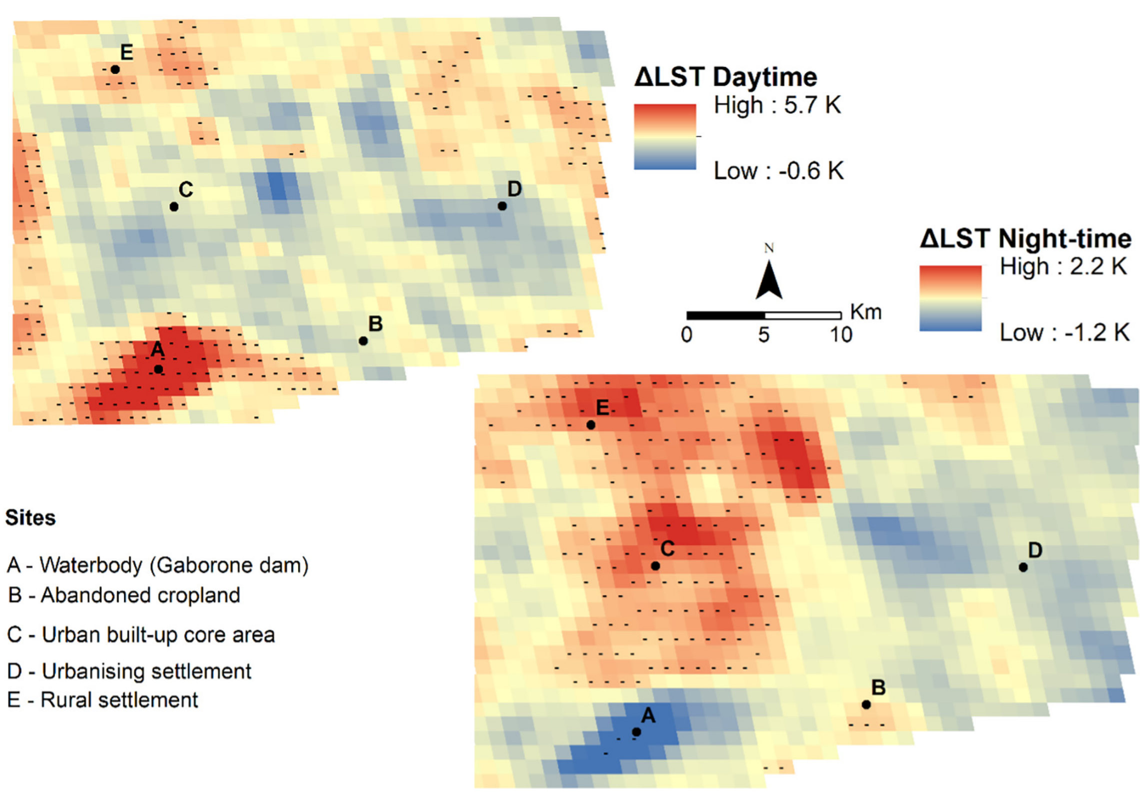

Fig. 3. Daytime and night-time LST trends in Kelvin (2000–2018) and assuming monotonic trends. Trends in pixels with a horizontal strip (–) are statistically significant at the 90% confidence level.

Table 3
Description and land cover characteristics for sites A to E.

Site	Coordinate	Cover/transition	Description
A – Gaborone dam	25.905003 −24.716490	Waterbody (persistence)	Impervious materials are used to create a reservoir for water storage in the Gaborone dam. The dam serves domestic, institutional, and industrial water supply to Gaborone and Lobatse located 72 km south of Gaborone city.
B – Abandoned cropland	26.033038 −24.695680	Cropland to grassland/tree-covered area	These are croplands with overgrowths to the south of Gaborone city and close to the South African border.
C – Urban	25.912632 −24.620127	Artificial surface (persistence)	Gaborone Extension 34 is a highly compact built-up commercial/industrial neighborhood.
D – Urbanizing	26.125890 −24.623460	Urbanizing, settlement expansion	Modipane is a small urbanizing settlement located 25 km east of Gaborone city. The area is surrounded by croplands and some deforested patches.
E – Rural	25.889671 −24.520864	Cropland and grassland exchanges	This area is in Letlhajweng, a rural agricultural landscape with predominantly croplands, grassland, and bare soils, to the northwest of Gaborone city.

commercial livestock farming [68]. The finding of increasing artificial surface areas due to settlement expansion is confirmed [33].

The findings that cropland decreased and tree-covered areas increased are not in line with the findings of Matlhodi et al. [33] which found that cropland increased and tree-covered areas decreased between 1984 and 2015. This disparity is mainly due to the different extent of the study locations. With a focus on urban LST, our study area comprised Gaborone city and the immediate surrounding up to the southern limit of the dam

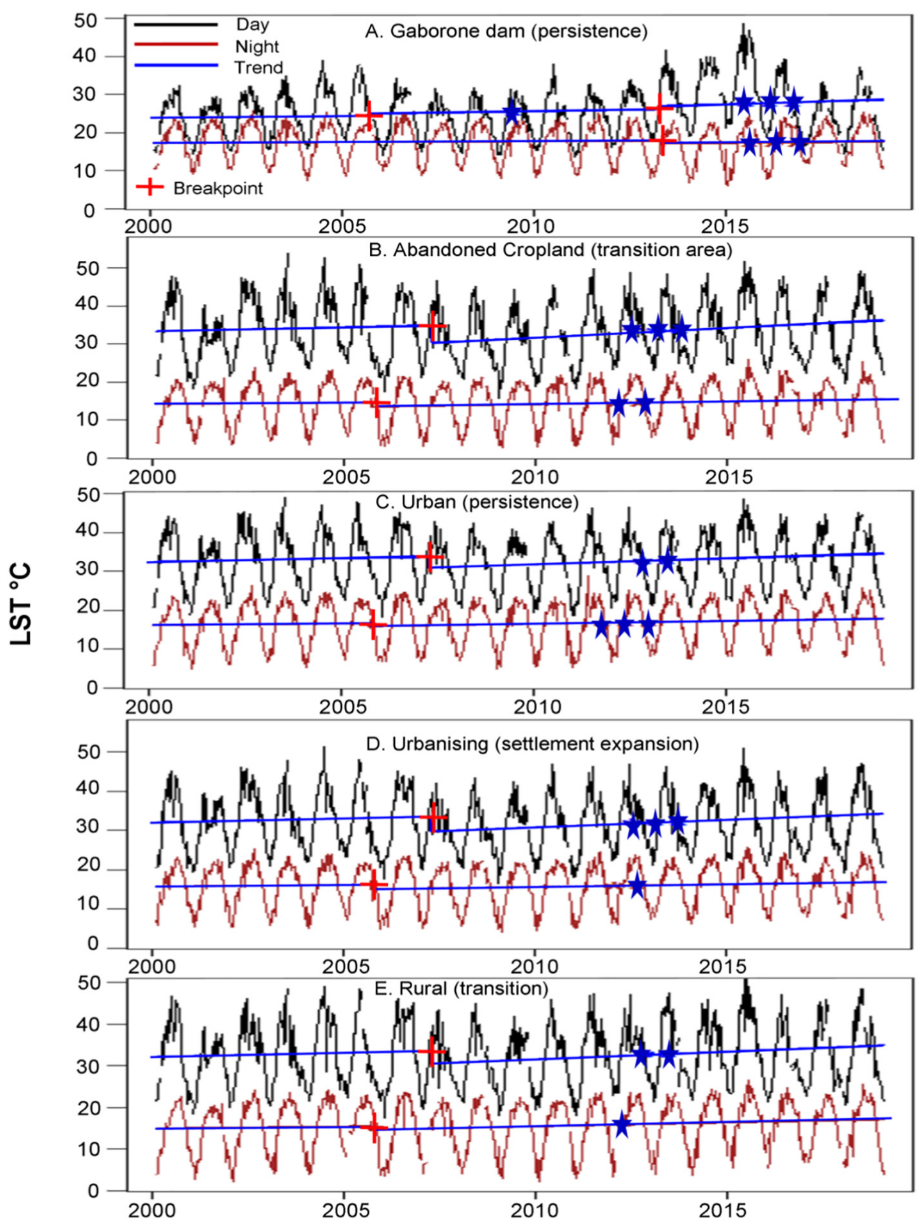

Fig. 4. Daytime and night-time LST trends and breakpoints for sites A to E. The *p*-value of each segment with a significant trend is indicated by the number of stars *** ($p \le 0.001$), ** ($p \le 0.01$), * ($p \le 0.05$), and no symbol if $p > 0.1$.

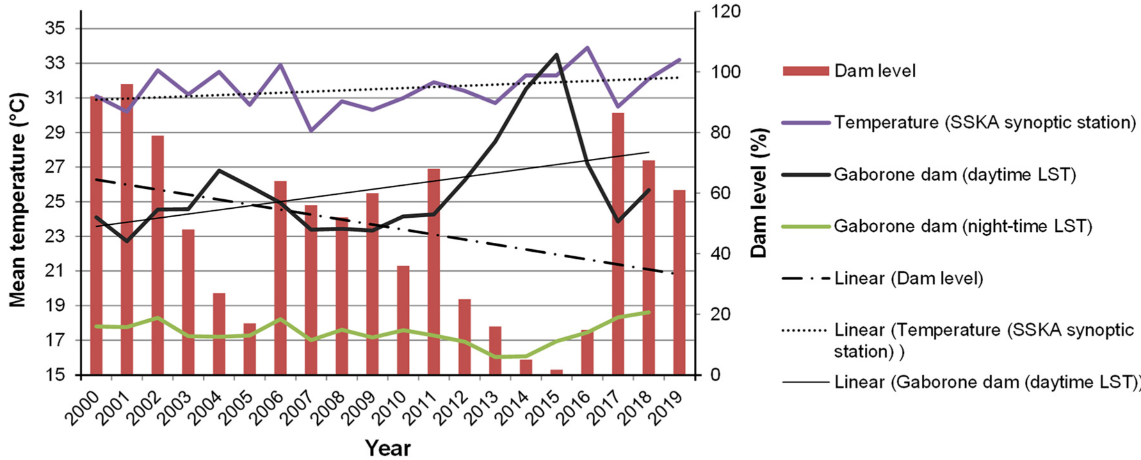

Fig. 5. Relating the Gaborone dam water level to temperature (MODIS daytime and night-time LST and synoptic station data). Sources: Dam water level data compiled from the following sources [[60–65]], SSKA temperature data from the Botswana Meteorological Services, LST from MOD11A2.006.

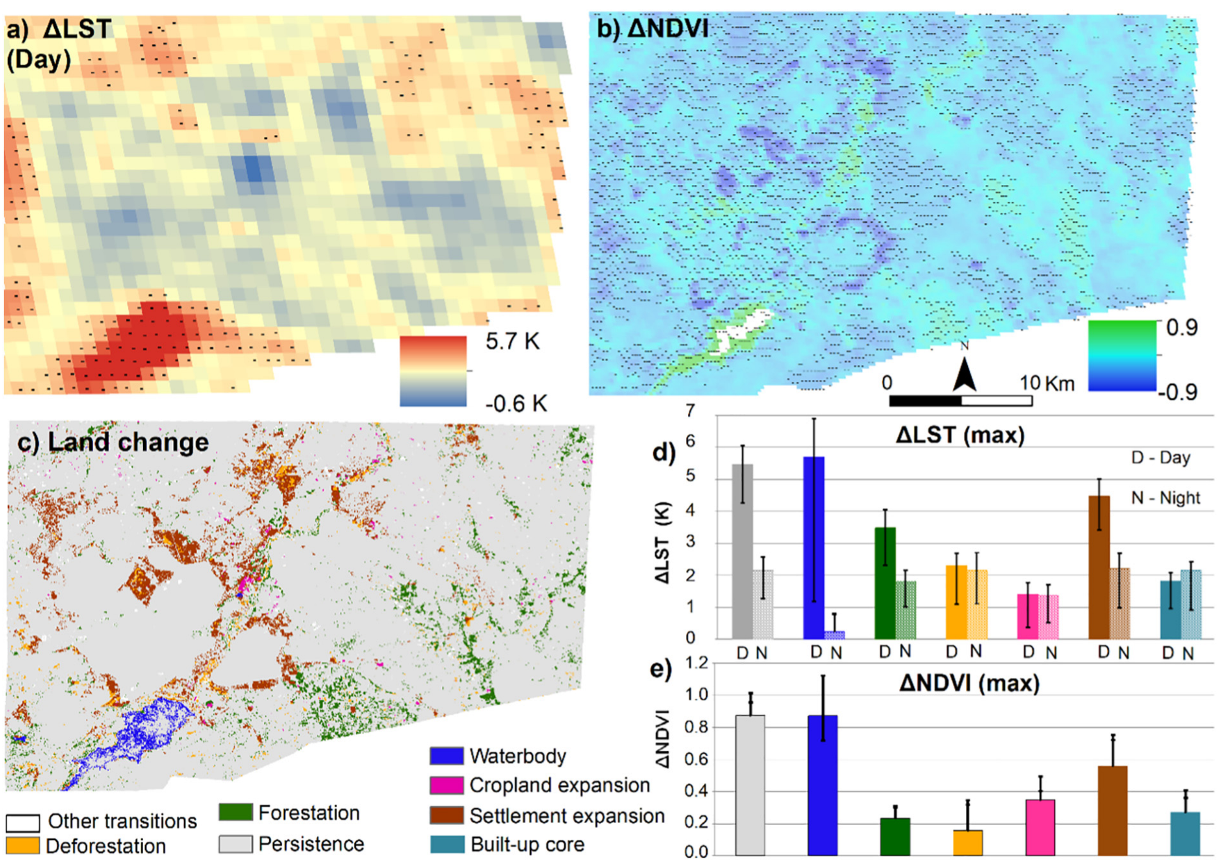

Fig. 6. Change in LST, NDVI (based on the STM model) and land cover in Gaborone between 2000 and 2018 are shown in a) to c) respectively. Trends in pixels with a horizontal strip (−) are statistically significant at the 90% confidence level. Maximum values of changes in LST (ΔLST daytime and night-time) and NDVI (ΔNDVI) in d) and e) were classified in terms of the land change (transitions) and persistent classes with σ and μ shown at the top and bottom of the error bars respectively.

Table 4
Statistics of the ΔLST and ΔNDVI.

	Min	Max	μ	σ
ΔLST	−0.55	5.69	1.21	0.65
ΔNDVI	−0.86	0.88	−8.14	0.10

Minimum (min), maximum (max), mean (μ), and standard deviation (σ).

reservoir (refer to Fig. 1), whereas they examined the Gaborone dam catchment, an area south of the dam excluding the city. To the south and southeast are patches of mostly croplands overgrown with shrubs and some areas of tree savannas. Visual inspection of high-resolution imagery confirms that many former croplands are now overgrown as they were left uncultivated, probably due to the recurrent droughts.

While applying the CVA minimizes error propagation from the PCC, certain false positives likely remained. For instance, the PCC flagged "new" waterbodies around the dam, products of flood dynamics. This is a false change that could not be entirely masked out with the CVA. The LST trends as well as the water table level (refer to Fig. 5) shows that there is indeed an overall decrease in water level. The increases in NDVI around the dam (Fig. 6b) seem to be a consequence of the growth of vegetation that the low water levels have allowed. Therefore, using biophysical indicators (e.g. LST, NDVI) can provide additional information on land cover trends and help to identify false changes, especially in complex and dynamic environments such as dams and/or natural wetlands in urbanizing contexts [19].

4.2. LST trends

Increasing daytime LST trends found over Gaborone built-up core areas (e.g. site C representing Gaborone Extension 34) were lower in magnitude when compared to night-time LST. Maximum daytime LST increases over the built-up areas were also lower than over the surrounding rural settlements with predominantly agricultural landscapes (e.g. site E Letlhajweng) or areas of settlement expansion. Decreasing trends in annual maximum temperature between 1985 and 2014 were found around the SSKA synoptic station, although not significant [69].

The rural areas surrounding Gaborone such as Letlhajweng (site E) have higher LST both during the day and at night than at Modipane (site D, urbanizing) where the increase in daytime and night-time LST remained low. The main difference between these two sites is that site E is predominantly an agricultural landscape with more bare soils and less vegetation, whereas site D is gradually urbanizing with built-up compactness although surrounded by cropland and grassland areas. Areas with bare soils and desert sands surrounding cities in dryland regions have been found with higher LST [25]. The variation in urban-rural minimum temperature patterns in Gaborone during the period 1994–1996, was attributed to the differences in urban and rural vegetation cover, particularly in winter [29]. Measures to reduce deforestation and exposure of bare soils are needed in urbanizing dryland regions.

Findings show the loss of most cropland areas within the city as these are converted into urban or abandoned. Daytime and night-time LST increases in cropland expansion areas are in line with previous researches [19]. However, milder increases in daytime LST than in night-time LST over some areas of cropland expansion may be because of irrigation such as at the Glen valley irrigation scheme (refer to Fig. 1) [70]. Similar patterns were found in China [71] where irrigation cooled down daytime LST more than night-time LST in arid zones, whereas the effects of irrigation in daytime and night-time LST were negligible in humid areas. Since Gaborone has since exceeded its planned limit of 20,000 inhabitants [35], the prospect for urban agriculture is very slim with the increasing loss of croplands within the city. Based on field observations, many residential buildings in Gaborone now have ornamental trees in the compound. In addition to providing shade, planting more fruit trees around buildings will increase access to fresh fruits for enhanced health of urban dwellers.

Increases in daytime LST were highest over the Gaborone Dam (site A), whereas night-time LST did not vary much across the study period. The two LST trend breakpoints detected over the dam in 2005 and 2013–2014 correspond to peaks in LST related to very low water levels. The first daytime LST trend breakpoint in 2005 was followed by floods in 2006 [65]. This explains the reduced LST values over the dam afterwards till 2013–2014 when a second breakpoint was detected, both in the daytime and night-time LST as the dam dried up [34]. Daytime LST variation over the dam seems to be mainly driven by the water level with which it is negatively correlated. Many factors affecting the dam water level include evaporation, increase in sediment load transported into the dam (which causes siltation), and reduced water inflow from the Notwane River catchment especially during droughts [33,72]. Water demand also increases as the population of Gaborone grows well beyond its 20,000 planned capacity [68].

All the monotonic significant trends we found for daytime and night-time LST were increasing over the study period, except for the LST over the Gaborone Dam, which depended more on the dam's water level. Increasing daytime and night-time LST trends, projected increasing temperature and drought frequency at varying global warming levels (GWL) mark this urbanizing dryland region out as being highly vulnerable. For example at 2.0 GWL, an increase in the number of hot nights and hot days by 8 to 9 days are projected over the region [73] as well as an increase in severe drought intensity and frequency of up to -1.0 and 2 event decade^{-1} respectively [31]. An LST trend breakpoint was often detected around 2006 (night-time) and 2007 (daytime), from where the increasing trends start. Note that a trend under the 90% confidence interval as was set in this study does not necessarily mean that there is no trend. For such a relatively short period covered by this study (18-years) and because of the several maxima found within this period, the location of the breakpoint might vary depending more on the parameters set rather than the actual data.

Even though the selected sites represent different land covers or transitions as evident from the NDVI trends, the LST patterns were similar except for the dam (refer to Fig. 4). The difference between the LST, NDVI and land cover change patterns might be partly explained by the different spatial resolutions of the datasets (1 km for the LST, 250 m for the NDVI, and 30 m for land cover). At coarser resolutions, it will be difficult to detect significant trends if the land cover changes took place at a finer scale. The similarity between the temporal patterns of the sites plotted in Fig. 4 suggests that for these types of dryland urbanizingscapes, climatic variables might explain a higher proportion of the variability of the LST than land cover changes. This also suggests a higher vulnerability of drylands to temperature change due to climatic events. For example, the daytime LST breakpoint from 2007 may be associated with the strong La Niña event in that year [60,74]. Additionally, in 2015 when daytime LST peaked over most sites, there was a very strong El Niño event [75]. The associated severe drought necessitated the official declaration of the year 2015 as a drought year by the government of Botswana [76]. Abundant storm waters brought about by Tropical Cyclone Dineo from the Indian Ocean may have contributed to the drop in daytime LST as observed during 2016/2017 [77].

5. Implications for sustainable urban land management and concluding remarks

Illustrated by the case of Gaborone, this study examined the effects of urban land cover change on LST by analyzing significant trends and breakpoints in daytime and night-time LST. The study area covered Gaborone City and its immediate surroundings to the southern limit of the Gaborone dam. Semi-arid Gaborone, as in many emerging African cities, is experiencing land cover changes driven by climatic changes, increasing population and consumption levels. Such cities in predominantly rural drylands in Africa and beyond must implement a wide range of adaptation options as the need to implement bioclimatic plans is higher in arid and semi-arid climatic regions.

For example, increasing nocturnal LST trends found in the built-up areas implies more energy will be required for cooling at night. Ameliorating the UHI condition to better improve the level of thermal comfort of city inhabitants is also important. With higher daytime and night-time LST found in areas of settlement expansion than the city core, better designs to mitigate increasing temperature are required in new development neighborhoods. New low-density housing developments in Erbil, Iraqi Kurdistan also had higher LST than in the urban core areas [27]. The role of parks, urban gardens and tree planting for shade around buildings in Gaborone ought to be explored. Studies such as Donovan and Butry [78] examined the impacts of trees on urban summertime electricity use in Sacramento, California and concluded that the effects of shade trees depend on which side of the building the trees were located. Urban gardens can also contribute to minimizing heat stress among urban dwellers and gardening is a good way to supply fresh produce from urban agriculture [79,80].

The built-up areas at the city core exhibited lower daytime LST increases than over the rural settlements and areas of settlement expansion.

Maximum night-time LST trends, however, showed inverse patterns as higher LST increases were found over the built-up areas than over the rural agricultural settlements. Although daytime and night-time LST trends increased over croplands, LST increases during the day were not as high as increases in night-time LST. This difference between daytime and night-time LST is probably due to irrigation of some croplands. Further study of the effects of irrigating croplands on urban LST in the study area is required.

All the daytime LST increases were highest over the Gaborone dam than elsewhere. Times in which the Gaborone dam dried up were picked up in the time series analysis as LST trend breakpoints in 2005 and 2013-2014 despite the coarse spatial resolution of MODIS LST (1 km). With daytime LST negatively correlated to the dam's water level, further analysis regarding the dam water level's influence on LST ought to be conducted in the future.

The high variability of LST when compared to NDVI, which appeared more stable, made it necessary to analyze the LST trends on a case by case basis. Apart from the Gaborone dam, most of the temporal LST patterns were very similar regardless of whether it was a land cover transition area or where a land cover type persisted. This finding suggests that for these types of urbanizing dryland landscapes, climatic variables might explain a proportion of the variability of the LST alongside land cover changes. Regardless, the loss of vegetation cover which increases bare soils and expansion of artificial surfaces (often with higher capacity to accumulate heat from the sun's radiation), will work synergistically with increases in temperature due to climate change.

Supplementary data to this article can be found online at https://doi.org/10.1016/j.cacint.2020.100029.

Funding

This research received no external funding.

CRediT authorship contribution statement

Felicia O. Akinyemi: Conceptualization, Methodology, Validation, Formal analysis, Investigation, Resources, Data curation, Writing - original draft, Writing - review & editing, Visualization, Supervision. **Mphoentle Ikanyeng:** Conceptualization, Methodology, Formal analysis, Investigation. **Javier Muro:** Methodology, Software, Formal analysis, Writing - review & editing.

Declaration of competing interest

The authors declare that they have no known competing financial interests or personal relationships that could have appeared to influence the work reported in this paper.

Acknowledgments

We are grateful for all datasets made freely available. Special thanks to the Botswana Department of Meteorological Services, Gaborone for the provision of the synoptic temperature data used in the study. The comments from the anonymous reviewers are highly appreciated.

References

[1] Deng Y, Wang S, Bai X, Tian Y, Wu L, Xiao J, et al. Relationship among land surface temperature and LUCC, NDVI in typical karst area. Sci Rep. 2018;8(1):641.
[2] Kopecká M, Nagendra H, Millington A. Urban land systems: an ecosystems perspective. Land. 2018;7(1):5.
[3] Li W, Cao Q, Lang K, Wu J. Linking potential heat source and sink to urban heat island: heterogeneous effects of landscape pattern on land surface temperature. Sci Total Environ. 2017;586:457–65.
[4] Mbow C. Africa's risky gamble. Global Change. 2010;75:20–3.
[5] Popp A, Calvin K, Fujimori S, Havlik P, Humpenöder F, Stehfest E, et al. Land-use futures in the shared socio-economic pathways. Glob Environ Chang. 2017;42:331–45.
[6] Vitousek PM. Human domination of Earth's ecosystems. Science. 1997;277(5325):494–9.
[7] Yu Y, Feng K, Hubacek K. Tele-connecting local consumption to global land use. Glob Environ Chang. 2013;23(5):1178–86.
[8] Gage EA, Cooper DJ. Relationships between landscape pattern metrics, vertical structure and surface urban heat island formation in a Colorado suburb. Urban Ecosyst. 2017;20(6):1229–38.
[9] Osborne PE, Alvares-Sanches T. Quantifying how landscape composition and configuration affect urban land surface temperatures using machine learning and neutral landscapes. Computers, Environment and Urban Systems. 2019;76:80–90.
[10] Akinbobola A. Simulating land cover changes and their impacts on land surface temperature in Onitsha, South East Nigeria. Atmospheric and Climate Sciences. 2019;9(2):243–63.
[11] Carter JG, Cavan G, Connelly A, Guy S, Handley J, Kazmierczak A. Climate change and the city: building capacity for urban adaptation. Progress in Planning. 2015;95:1–66.
[12] Wang W, Liang S, Meyers T. Validating MODIS land surface temperature products using long-term nighttime ground measurements. Remote Sens Environ. 2008;112(3):623–35.
[13] Xie M, Wang Y, Chang Q, Fu M, Ye M. Assessment of landscape patterns affecting land surface temperature in different biophysical gradients in Shenzhen. China Urban Ecosystems. 2013;16(4):871–86.
[14] Turner II BL. Land system architecture for urban sustainability: new directions for land system science illustrated by application to the urban heat island problem. J Land Use Sci. 2016;11(6):689–97.
[15] Tarawally M, Xu W, Hou W, Mushore T. Comparative analysis of responses of land surface temperature to long-term land use/cover changes between a coastal and Inland City: a case of Freetown and Bo Town in Sierra Leone. Remote Sens (Basel). 2018;10(1):112.
[16] Ayansina A, Howard MT. Land surface temperature and heat fluxes over three cities in Niger Delta. Journal of African Earth Sciences. 2019;151:54–66. https://doi.org/10.1016/j.jafrearsci.2018.11.027.
[17] Mushore TD, Dube T, Manjowe M, Gumindoga W, Chemura A, Rousta I, et al. Remotely sensed retrieval of Local Climate Zones and their linkages to land surface temperature in Harare metropolitan city, Zimbabwe. Urban Climate. 2019;27:259–71. https://doi.org/10.1016/j.uclim.2018.12.006.
[18] Abdramane D, Ye X, Amadou T. Analysis of land surface temperature change based on MODIS data, case study: Inner Delta of Niger. Nat Hazards Earth Syst Sci Discuss. 2018. https://doi.org/10.5194/nhess-2018-208.
[19] Muro J, Strauch A, Heinemann S, Steinbach S, Thonfeld F, Waske B, et al. Land surface temperature trends as indicator of land use changes in wetlands. International Journal of Applied Earth Observation and Geoinformation. 2018;70:62–71.
[20] Akinyemi FO, Pontius Jr RG, Braimoh AK. Land change dynamics: insights from Intensity Analysis applied to an African emerging city. Journal of Spatial Science. 2017;62(1):69–83. https://doi.org/10.1080/14498596.2016.1196624.
[21] Christopherson RW. Geosystems: an introduction to physical geography. New Jersey, USA: Pearson Prentice Hall; 2012.
[22] Cobbinah PB, Darkwah RM. African urbanism: the geography of urban greenery. Urban Forum. 2016;27(2):149–65.
[23] Göpfert C, Wamsler C, Lang W. Institutionalizing climate change mitigation and adaptation through city advisory committees: lessons learned and policy futures. City and Environment Interactions. 2019;1:100004.
[24] Simon D, Leck H. Understanding climate adaptation and transformation challenges in African cities. Curr Opin Environ Sustain. 2015;13:109–16.
[25] Rasul A, Balzter H, Smith C, Remedios J, Adamu B, Sobrino JA, et al. A review on remote sensing of urban heat and cool islands. Land. 2017;6:38. https://doi.org/10.3390/land6020038.
[26] Fu P, Weng Q. A time series analysis of urbanization induced land use and land cover change and its impact on land surface temperature with Landsat imagery. Remote Sens Environ. 2016;175:205–14. https://doi.org/10.1016/j.rse.2015.12.040.
[27] Rasul A, Balzter H, Smith C. Spatial variation of the daytime Surface Urban Cool Island during the dry season in Erbil, Iraqi Kurdistan, from Landsat 8. Urban Clim. 2015;14(2):176–86. https://doi.org/10.1016/j.uclim.2015.09.001.
[28] Sobrino JA, Julien Y, García-Monteiro S. Surface temperature of the planet earth from satellite data. Remote Sens (Basel). 2020;12:218.
[29] Jonsson P. Vegetation as an urban climate control in the subtropical city of Gaborone, Botswana. International Journal of Climatology. 2004;24(10):1307–22.
[30] Akinyemi FO, Mashame G. Analysis of land change in the dryland agricultural landscapes of eastern Botswana. Land Use Policy. 2018;76:798–811. https://doi.org/10.1016/j.landusepol.2018.03.010.
[31] Akinyemi FO, Abiodun BJ. Potential impacts of global warming levels 1.5 °C and above on climate extremes in Botswana. Clim Change. 2019;154(3–4):387–400. https://doi.org/10.1007/s10584-019-02446-1.
[32] Ministry of Land Management, Water and Sanitation Services. Botswana water accounting report 2015–2016. Department of Water Affairs 2017, Gaborone, Botswana. (36 pp.).
[33] Matlhodi B, Kenabatho PK, Parida BP, Maphanyane JG. Evaluating land use and land cover change in the Gaborone dam catchment, Botswana, from 1984–2015 using GIS and remote sensing. Sustainability. 2019;11(19):5174.
[34] Central Statistics Office. Botswana statistical yearbook. Gaborone, Botswana: Central Statistics Office; 2011.
[35] Mgadla T. A very grave and expensive error? The legislative council's debate on the choice of a new site for the capital of Botswana, 1961–1965. Botswana Notes and Records. 2017;48:61–71.
[36] Gomis-Cebolla J, Jiménez-Muñoz J, Sobrino J. MODIS-based monthly LST products over Amazonia under different cloud mask schemes. Data. 2016;1(2):2.
[37] Julien Y, Sobrino JA, Mattar C, Ruescas AB, Jiménez-Muñoz JC, Sòria G, et al. Temporal analysis of normalized difference vegetation index (NDVI) and land surface temperature (LST) parameters to detect changes in the Iberian land cover between 1981 and 2001. International Journal of Remote Sensing. 2011;32(7):2057–68.

[38] Keramitsoglou I, Kiranoudis CT, Ceriola G, Weng Q, Rajasekar U. Identification and analysis of urban surface temperature patterns in Greater Athens, Greece, using MODIS imagery. Remote Sens Environ. 2011;115(12):3080–90.
[39] Neteler M. Estimating daily land surface temperatures in mountainous environments by reconstructed MODIS LST data. Remote Sens (Basel). 2010;2(1):333–51.
[40] Wongsai N, Wongsai S, Huete A. Annual seasonality extraction using the cubic spline function and decadal trend in temporal daytime MODIS LST data. Remote Sens (Basel). 2017;9(12):1254.
[41] Ghazaryan G, Dubovyk O, Kussul N, Menz G. Towards an improved environmental understanding of land surface dynamics in Ukraine based on multi-source remote sensing time-series datasets from 1982 to 2013. Remote Sens (Basel). 2016;8(8): 617.
[42] Leroux L, Bégué A, Seen DL, Jolivot A, Kayitakire F. Driving forces of recent vegetation changes in the Sahel: lessons learned from regional and local level analyses. Remote Sens Environ. 2017;191:38–54.
[43] Forkel M, Carvalhais N, Verbesselt J, Mahecha M, Neigh C, Reichstein M. Trend change detection in NDVI time series: effects of inter-annual variability and methodology. Remote Sens (Basel). 2013;5(5):2113–44. https://doi.org/10.3390/rs5052113.
[44] Verbesselt J, Hyndman R, Newnham G, Culvenor D. Detecting trend and seasonal changes in satellite image time series. Remote Sens Environ. 2010;114(1):106–15.
[45] Holben BN. Characteristics of maximum-value composite images from temporal AVHRR data. International Journal of Remote Sensing. 1986;7(11):1417–34.
[46] Mattina D, Erdogan HE, Wheeler I, Crossman ND, Cumani R, Minelli S. Default data: methods and interpretation. A guidance document for the 2018 UNCCD reporting. [accessed 2020 January 25]. https://prais.unccd.int/sites/default/files/helper_documents/3-DD_guidance_EN.pdf; 2018.
[47] Penman J, Gytarsky M, Hiraishi T, Krug T, Kruger D, Pipatti R, et al. September 26. IPCC good practice guidance for land use, land-use change and forestry. Available online: https://www.ipcc-nggip.iges.or.jp/public/gpglulucf/gpglulucf_files/GPG_LULUCF_FULL.pdf; 2003. (accessed on 12 January 2020).
[48] Santoro M, Kirches G, Wevers J, Boettcher M, Brockmann C, Lamarche C, et al. Land Cover CCI product user guide version 2.0. Available online: https://maps.elie.ucl.ac.be/CCI/viewer/download/ESACCI-LC-Ph2-PUGv2_2.0.pdf. (accessed on 17 April 2019).
[49] Jonckheere I, Nackaerts K, Muys B, Lambin E. Digital change detection methods in ecosystem monitoring: a review. International Journal of Remote Sensing. 2004;25: 1565–96.
[50] Drakopoulos V, Nikolaou NP. Efficient computation of the Hutchinson metric between digitized images. IEEE Trans Image Process. 2004;13(12):1581–8.
[51] Hecheltjen A, Thonfeld F, Menz G. Recent advances in remote sensing change detection – a review. In: Manakos I, Braun M, editors. Land use and land cover mapping in Europe. Dordrecht Netherlands: Springer; 2014. p. 145–78.
[52] Malila WA. Change vector analysis: An approach for detecting forest changes with Landsat. Proceedings of the LARS Symposia, West Lafayette, IN, USA, 385. ; 3–6 June 1980. p. 326–35.
[53] Thonfeld F, Steinbach S, Muro J, Kirimi F. Long-term land use/land cover change assessment of the Kilombero catchment in Tanzania using random Forest classification and robust change vector analysis. Remote Sens (Basel). 2020;12:1057. https://doi.org/10.3390/rs12071057.
[54] Tucker CJ. Red and photographic infrared linear combinations for monitoring vegetation. Remote Sens Environ. 1979;8(2):127–50.
[55] McFeeters SK. The use of the normalized difference water index (NDWI) in the delineation of open water features. International Journal of Remote Sensing. 1996;17(7): 1425–32.
[56] Zha Y, Gao J, Ni S. Use of normalized difference built-up index in automatically mapping urban areas from TM imagery. International Journal of Remote Sensing. 2003;24 (3):583–94.
[57] Mack B, Leinenkugel P, Kuenzer C, Dech S. A semi-automated approach for the generation of a new land use and land cover product for Germany based on Landsat time-series and Lucas *in-situ* data. Remote Sensing Letters. 2017;8(3):244–53.
[58] Otsu N. A threshold selection method from gray-level histograms. IEEE Trans Syst Man Cybern. 1979;9:62–6. https://doi.org/10.1109/TSMC.1979.4310076.
[59] Dash P, Göttsche FM, Olesen FS, Fischer H. Land surface temperature and emissivity estimation from passive sensor data: theory and practice-current trends. International Journal of Remote Sensing. 2002;23(13):2563–94.
[60] Batlotleng B. Gaborone dam overflows after 10 years. Daily news of 26 February 2017. Available online: http://www.dailynews.gov.bw/news-details.php?nid=34266. (accessed on 08 January 2020).
[61] Botswana Water Utilities Corporation (BWUC). Dam levels. Available online: https://www.wuc.bw/wuc-content/id/351/dam-levels/. (accessed on 08 January 2020).
[62] Chanda R, Mosetlhi BT, Sakuringwa S, Makwati M. Water for urban development or rural livelihoods: is that the question for Botswana's Notwane River catchment. Botswana Notes and Records. 2018;50:1385.
[63] Ministry of Minerals, Energy and Water resources. Dam levels and water supply situation. Available online: http://www.gov.bw/en/Ministries–Authorities/Ministries/Ministry-of-Minerals-Energy-and-Water-Resources-MMWER/News-and-Press-Releases/DAM-LEVELS-AND-WATER-SUPPLY-SITUATION–241020132/. (accessed on 25 December 2019).
[64] Statistics Botswana. Botswana environemt statistics: natural disasters digest 2015. Available online: http://www.statsbots.org.bw/sites/default/files/publications/Botswana%20Environment%20Natural%20Disasters%20Digest%202015.pdf. (accessed on 25 December 2019).
[65] Sunday Standard. The rich blocking water flow into Gaborone dam; a rejoinder. Available online: https://www.sundaystandard.info/the-rich-blocking-water-flow-into-gaborone-dam-a-rejoinder/; February 2, 2014. (accessed on 29 December, 2019).
[66] Liu K, Su H, Li X, Wang W, Yang L, Liang H. Quantifying spatial–temporal pattern of urban heat island in Beijing: an improved assessment using land surface temperature (LST) time series observations from Landsat, MODIS, and Chinese new satellite GaoFen-1. IEEE Journal of Selected Topics in Applied Earth Observations and Remote Sensing. 2016;9(5):2028–42. https://doi.org/10.1109/JSTARS.2015.2513598.
[67] Wang S, Ma Q, Ding H, Liang H. Detection of urban expansion and land surface temperature change using multi-temporal Landsat images. Resources, Conservation and Recycling. 2018;128:526–34. https://doi.org/10.1016/j.resconrec.2016.05.011.
[68] Sebego RJ, Gwebu TD. Patterns, determinants, impacts and policy implications of the spatial expansion of an African capital city: the Greater Gaborone example. Int J Sustain Built Environ. 2013;2(2):193–208.
[69] Byakatonda J, Parida BP, Kenabatho PK, Moalafhi DB. Analysis of rainfall and temperature time series to detect long-term climatic trends and variability over semi-arid Botswana. J Earth Syst Sci. 2018;127:25. https://doi.org/10.1007/s12040-018-0926-3.
[70] Dikinya O, Areola O. Comparative assessment of heavy metal concentration in treated wastewater irrigated soils cultivated to different crops in the Glen Valley. Botswana Afr Crop Sci Conf Proc. 2009;9:351–5. https://doi.org/10.1007/BF03326143.
[71] Yang Q, Huang X, Tang Q. Irrigation cooling effect on land surface temperature across China based on satellite observations. Sci Total Environ. 2020;705:135984. https://doi.org/10.1016/j.scitotenv.2019.135984.
[72] Kadibadiba AT. A city in a water crisis: the responses of the people of Gaborone. Master thesis in applied science at Lincoln University, Christchurch, New Zealand; 2017 Available online: https://researcharchive.lincoln.ac.nz/bitstream/handle/10182/8149/Kadbadiba_MApplSc.pdf?sequence=1&isAllowed=y. (accessed 12 January 2020).
[73] Nkemelang T, New M, Zaroug MAH. Temperature and precipitation extremes under current, 1.5°C and 2.0°C global warming above pre-industrial levels over Botswana, and implications for climate change vulnerability. Environ Res Lett. 2018;13(6):065016. https://doi.org/10.1088/1748-9326/aac2f8.
[74] Abdi AM, Vrieling A, Yengoh GT, Anyamba A, Seaquist JW, Ummenhofer CC, et al. The El Niño – La Niña cycle and recent trends in supply and demand of net primary productivity in African drylands. Clim Change. 2016;138(1–2):111–25. https://doi.org/10.1007/s10584-016-1730-1.
[75] Food and Agricultural Organisation. Delayed onset of seasonal rains in parts of southern Africa raises serious concern for crop and livestock production in 2016. Special alert for Southern Africa 336, pp. 6. 2015 Available online: http://www.fao.org/3/a-i5258e.pdf (accessed 12 January 2020).
[76] Akinyemi FO. Climate change and variability in semiarid Palapye, eastern Botswana: an assessment from smallholder farmers' perspective. Weather, Climate, and Society. 2017; 9(3):349–65. https://doi.org/10.1175/WCAS-D-16-0040.1.
[77] Disaster Relief Emergency Fund DREF. Emergency plan of action preliminary final report Botswana: floods. Available online: https://reliefweb.int/sites/reliefweb.int/files/resources/MDRBW003dfr_preliminary.pdf; 2017. (accessed on 08 January 2020).
[78] Donovan GH, Butry DT. The value of shade: estimating the effect of urban trees on summertime electricity use. Energ Buildings. 2009;41:662–8. https://doi.org/10.1016/j.enbuild.2009.01.002.
[79] Ma S, Pitman A, Yang J, Carouge C, Evans JP, Hart M, et al. Evaluating the effectiveness of mitigation options on heat stress for Sydney, Australia. J Appl Meteor Climatol. 2018; 57:209–20. https://doi.org/10.1175/JAMC-D-17-0061.1.
[80] Barbierato E, Bernetti I, Capecchi I, Saragosa C. Quantifying the impact of trees on land surface temperature: a downscaling algorithm at city-scale. European Journal of Remote Sensing. 2019;52(sup4):74–83. https://doi.org/10.1080/22797254.2019.1646104.